Longitudinal Changes in Functional Connectivity of Cortico-Basal Ganglia Networks in Manifests and Premanifest Huntington's Disease

Fatma Gargouri,[1,2,3] Arnaud Messé,[4,5] Vincent Perlbarg,[1,5,6]
Romain Valabregue,[1,2] Peter McColgan,[7] Lydia Yahia-Cherif,[1,2]
Sara Fernandez-Vidal,[1,2] Ahmed Ben Hamida,[3] Habib Benali,[5]
Sarah Tabrizi,[7] Alexandra Durr,[2,8] and Stéphane Lehéricy[1,2,9,10]*

[1]Institut Du Cerveau Et De La Moelle Épinière – ICM, Centre De NeuroImagerie De Recherche – CENIR, Paris, France
[2]Institut Du Cerveau Et De La Moelle Épinière – ICM, Sorbonne Universités, UPMC Univ Paris 06, Inserm U1127, CNRS UMR 7225, Paris, France
[3]Advanced Technologies for Medicine and Signals – ATMS, Ecole Nationale D'Ingénieurs De Sfax – ENIS, Sfax Université, Tunisia
[4]Department of Computational Neuroscience, University Medical Center Eppendorf, Hamburg University, Germany
[5]Sorbonne Universités, UPMC Univ Paris 06, CNRS UMR 7371, Inserm UMR_S 1146, Laboratoire D'Imagerie Biomédicale, Paris, F-75013, France
[6]Bioinformatics and Biostatistics platform - ICONICS, Institut Du Cerveau Et De La Moelle Épinière – ICM, Paris, France
[7]Department of Neurodegenerative Disease, UCL Institute of Neurology, London, WC1N 3BG, UK
[8]Department of Genetics, APHP, University Hospital Pitié-Salpêtrière, Paris, France
[9]ICM Team Control of Normal and Abnormal Movement
[10]Groupe Hospitalier Pitié-Salpêtrière, Service De Neuroradiologie, Paris, France

◆━━━━━━━━━━━━━━━━━━━━━━━━━━━━━━━━◆

Abstract: Huntington's disease (HD) is a genetic neurological disorder resulting in cognitive and motor impairments. We evaluated the longitudinal changes of functional connectivity in sensorimotor, associative and limbic cortico-basal ganglia networks. We acquired structural MRI and resting-state fMRI in three visits one year apart, in 18 adult HD patients, 24 asymptomatic mutation carriers (preHD) and 18 gender- and age-matched healthy volunteers from the TRACK-HD study. We inferred topological

changes in functional connectivity between 182 regions within cortico-basal ganglia networks using graph theory measures. We found significant differences for global graph theory measures in HD but not in preHD. The average shortest path length (L) decreased, which indicated a change toward the random network topology. HD patients also demonstrated increases in degree k, reduced betweeness centrality bc and reduced clustering C. Changes predominated in the sensorimotor network for bc and C and were observed in all circuits for k. Hubs were reduced in preHD and no longer detectable in HD in the sensorimotor and associative networks. Changes in graph theory metrics (L, k, C and bc) correlated with four clinical and cognitive measures (symbol digit modalities test, Stroop, Burden and UHDRS). There were no changes in graph theory metrics across sessions, which suggests that these measures are not reliable biomarkers of longitudinal changes in HD. preHD is characterized by progressive decreasing hub organization, and these changes aggravate in HD patients with changes in local metrics. HD is characterized by progressive changes in global network interconnectivity, whose network topology becomes more random over time. *Hum Brain Mapp 37:4112–4128, 2016.*   © 2016 **Wiley Periodicals, Inc.**

Key words: cortico-basal ganglia networks; graph theory; Huntington's disease; resting-state functional MRI

◆━━━━━━━━━━━━━━━━━━━━━━━━━━◆

INTRODUCTION

Huntington's disease (HD) is an autosomal dominant genetic neurological disorder caused by a cytosine-adenine–guanine (**CAG**) trinucleotide expansion on chromosome 4 in the first exon of the huntingtin gene. Clinically, HD is characterized by motor, cognitive and behavioral disturbances. Neuronal loss in HD predominates in the basal ganglia (striatum and globus pallidus) [Vonsattel, 2008] but also affects the cortex and occurs several years prior to the onset of motor symptoms [Tabrizi et al., 2009]. Individuals who satisfy the genetic criteria for HD but do not yet show unequivocal motor signs are in the prodromal phase of the disease (preHD).

In preHD subjects, neuroimaging has revealed reduced brain volume or thickness and abnormal shapes that begin in the basal ganglia and extend to the cortex [Tabrizi et al., 2009]. Structural MRI can detect changes in volume [Majid et al., 2011] or shape of the brain [Dumas et al., 2012; Tabrizi et al., 2009] over 1 year in preHD subjects. Higher atrophy rates are observed in the basal ganglia than in the cortex [Ross and Tabrizi, 2011]. Clinical changes have been related to structural changes. The heterogeneity of HD symptoms is suggested to result from the dysfunction of

distinct cortico-basal ganglia circuits [Delmaire et al., 2013], which is likely due to neuronal loss in the cortex and basal ganglia and abnormal connections within cortico-basal ganglia networks. Structural neuroimaging studies have shown that functionally segregated sensorimotor, associative and limbic cortico-basal ganglia networks may specifically contribute to clinical expressions of HD comprising motor, cognitive or psychiatric comorbidities, respectively [Delmaire et al., 2013; Rosas et al., 2005; Teichmann et al., 2005].

It is less clear how the degenerative process influences the pattern of functional connections among anatomical regions and leads to symptom expression. Resting-state functional MRI (rs-fMRI) connectivity measures the synchronization in slow blood oxygen level dependent (BOLD) signal fluctuations between different brain regions at rest and is a potential tool to study abnormal brain function and its relation with changes in brain structure and symptom expression [Damoiseaux and Greicius, 2009; Fornito et al., 2015]. The intrinsic activity at rest may reflect some aspects of the functional capacity of neural systems and can consequently be considered appropriate for studying brain function [Greicius et al., 2009]. The characterization of spontaneous brain functional networks and analysis of rs-fMRI data can be performed using numerous different methods that employ region-based or whole-brain approaches such as independent component analysis or graph theory, which is a more recent development [Bullmore and Sporns, 2009]. Graph theory suggests that brain networks are organized according to small-world architecture defined by high clustering of functionally related areas with short average path lengths [Bullmore and Sporns, 2012]. This organization is suggested to satisfy the competitive demands of brain networks in local and global information processing [Kaiser and Hilgetag, 2006].

Abbreviations

BA	Brodmann area
BOLD	blood oxygen level dependent
CAG	cytosine–adenine–guanine
HD	Huntington's disease
preHD	premanifest HD
ROI	region of interest
rs-fMRI	resting-state functional MRI
SD	standard deviation
SDMT	symbol digit modalities test;
UHDRS	Huntington's disease rating scale

In HD, most functional imaging studies have reported reduced functional connectivity at rest within motor areas as well as associative areas of the frontal and parietal lobes [Dumas et al., 2013; Poudel et al., 2014], the basal ganglia [Werner et al., 2014] and the default mode network [Dumas et al., 2013]. In preHD, reduced connectivity has been reported in the same networks [Dumas et al., 2013; Koenig et al., 2014; Poudel et al., 2014; Unschuld et al., 2012], as well as in the visual system [Poudel et al., 2014]. Using graph theory, a recent study suggested that network properties approximated the random topology in preHD [Harrington et al., 2015]. This study also revealed weakened fronto-striatal connections with strengthened fronto-posterior connections that evolved as burden increased [Harrington et al., 2015]. Two longitudinal studies investigated preHD and assessed the potential utility of rs-fMRI as a biomarker of disease progression [Odish et al., 2015; Seibert et al., 2012]. These two studies did not find significant changes in connectivity over a one-year [Seibert et al., 2012] or a three-year period [Odish et al., 2015].

In this study, we evaluated the changes in functional organization within the sensorimotor, associative and limbic cortico-basal ganglia networks in preHD and HD patients compared with controls using rs-fMRI and graph theory over a 2-year period. We compared functional changes with changes in brain structures in the basal ganglia of these subjects by calculating Pearson's correlations between volumes and graph theory metrics of the basal ganglia. We also investigated whether specific functional nodes or circuits contributed to the severity and variability of the clinical outcome.

MATERIALS AND METHODS

Subjects

A total of 30 adult manifest HD patients (HD), 32 premanifest gene carriers (preHD) and 30 healthy volunteers (HV) were included at the Paris site (Institut du Cerveau et la Moelle epinière, France) in the frame of the longitudinal TRACK-HD study from 2008 to 2010. Of these participants, 10 HD, 7 preHD patients and 8 HV were excluded from the study because as they did not complete all three visits. Another 2 HD, 1 preHD and 4 HV patients were excluded from the study because of poor MRI quality due to excessive head motion during scanning (as defined below). A total of 18 HD, 24 preHD and 18 HV patients who had completed all three visits with good-quality MRI data were included in the fMRI analysis. The HD patients, preHD patients and HV were matched for age (ANOVA, P-value = 0.49) and gender (P-value = 0.70, χ^2 test) (Table I). The study was approved by the local ethics committee, and all of the participants provided written, informed consent prior to participating in the study.

The clinical assessment, which was performed according to the TRACK-HD standards, included the Unified Huntington's Disease Rating Scale (UHDRS-99) [Unified Huntington's Disease Rating Scale, 1996], a medical and psychiatric history, current medications, HD history, clinical motor scores, portions of the cognitive component (symbol digit modalities test [SDMT]) [Smith, 1982], the Stroop Word test [Stroop, 1935] and functional capacity. The HV had no history of neurological or psychiatric disease, no contraindications for MRI and no HD inclusion criteria. The inclusion criteria for the HD patients included a positive genetic test for the HTT gene with 40 or more CAG repeats. Furthermore, the HD patients had scores higher than five points on the UHDRS and a total functional capacity score greater than or equal to seven points. The inclusion criteria for the preHD subjects consisted of a positive genetic test with ≥40 CAG repeats and the absence of motor disturbances with five or fewer points on the UHDRS-TMS. Finally, a burden score ([CAG repeat length-35.5] × age) exceeding 250 was required [Penney et al., 1997]. Additional exclusion criteria included clinical evidence of unstable medical or psychiatric illness, the use of prescription antipsychotic medications within the past 6 months, the use of phenothiazine-derivative antiemetic medications more than three times per month, alcohol or drug abuse within the past year, history of another neurological condition, or an inability to undergo MRI scanning. Subjects participating in the longitudinal TRACK-HD study underwent MRI scanning at three time points (over two years).

Image Acquisition

The data were acquired using a 3T Siemens Trio TIM MRI scanner with body coil excitation and a 12-channel receive-phased-array head coil (CENIR, ICM, Paris, France).

We acquired anatomical scans using sagittal three-dimensional T1-weighted magnetization-prepared rapid acquisition gradient echo acquisition (field of view = 256 × 256 mm^2; repetition time (TR) = 2,200 ms, echo time (TE) = 2.9 ms, flip angle = 10°, voxel size = 1 × 1 × 1 mm^3).

We acquired functional MRI data of the whole brain using a gradient echo echo-planar imaging sequence sensitive to the BOLD signal (field of view = 64 × 64 × 45 mm^3; TR = 2,400 ms, TE = 30 ms; flip angle = 90°, 200 volumes in one session; voxel size = 3 × 3 × 3 mm^3, no gap).

The rs-fMRI data were acquired over the course of 6 min. During the scans, the subjects were instructed to relax, refrain from any structured thoughts and keep their eyes closed and not fall asleep. This isolated the intrinsic variations of the BOLD signal of the nervous system in subjects performing no particular task. Each subject underwent an MRI examination at each of the three visits separated by one year (baseline: 2008, year 1: 2009, year 2: 2010).

TABLE I. Clinical characteristics of participants and cognitive variables UHDRS-99 (Unified Huntington Disease Rating Scale), SDMT (Symbol Digit Modalities test), Stroop Word test

		HV	preHD	HD	P-value	Post hoc t-test (P-value)
Demographics						
Number of subjects		24	18	18		
Males/females		09/09	06/12	16/13		
Age (years)		44.0 ± 10.1	38.6 ± 9.1	51.3 ± 7.4	0.7	
CAG repeats		—	43.34 ± 2.06	42.28 ± 1.71	0.49	
Disease characteristics						
BDI		—	8.6 ± 10.1	13.1 ± 11.1		
TFC		—	13.0 ± 0.0	12.1 ± 1.6		
Burden		—	302.6 ± 40.2	346.9 ± 82.9		
Cognitive and clinical variables					ANOVA Mixed model F value (P-value)	
UHDRS	S1	1.7 ± 0.2	2.7 ± 0.4	19.5 ± 1.8	Group effect 86.36 (0)	HV<HD in S1, S2, S3 ($P < 0.01$)
	S2	1.5 ± 0.3	4.4 ± 0.8	21.7 ± 1.8	Session effect 8.73 (0.0002)	HV<preHD in S2, S3 ($P < 0.01$)
	S3	2.2 ± 0.4	6.0 ± 0.9	22.4 ± 1.5	Interaction 1.67 (0.15)	preHD<HD in S1, S2, S3 ($P < 0.01$); preHD S1<S3 ($P = 0.01$)
SDMT	S1	53.2 ± 1.2	47.4 ± 1.9	32.1 ± 1.5	Group effect 55.08 (4×10^{-15})	HV>HD in S1, S2, S3 ($P < 0.01$)
	S2	54.9 ± 1.2	49.1 ± 1.8	29.7 ± 1.6	Session effect 0.22 (0.79)	HV>preHD in S1, S2, S3 ($P < 0.01$)
	S3	55.4 ± 1.4	49.5 ± 2.2	28.8 ± 1.6	Interaction 5.07 (0.0007)	preHD>HD in S1, S2, S3 ($P < 0.01$)
STROOP	S1	108.2 ± 3.3	101.0 ± 2.7	85.0 ± 3.3	Group effect 19.25 (2×10^{-7})	HV>HD in S1, S2, S3 ($P < 0.01$)
	S2	113.0 ± 3.0	108.2 ± 3.1	84.4 ± 3.3	Session effect 7.95 (0.0005)	HV>preHD in S1, S2, S3 ($P < 0.01$)
	S3	114.8 ± 2.8	106.1 ± 2.7	81.9 ± 3.6	Interaction 5.18 (0.006)	

Functional Image Preprocessing

We first looked for differences in head motion between the three groups. For each session in each subject, we calculated the framewise displacement (FD) from Power et al. [2014], an index which yields a six dimensional time-series that represents instantaneous head motion. We excluded seven subjects with excessive head motion in at least one of the three sessions [FD > 0.5 mm as defined in Power et al. 2014]. We additionally performed subjective visual quality control on all of the scans to ensure correct registration. In the remaining 60 subjects × three sessions (180 MRI examinations), Kruskal Wallis test showed no statistically significant differences in head motion among groups as shown by the mean estimated FD values: 0.17 ± 0.07 mm in HD, 0.16 ± 0.08 mm in preHD and 0.15 ± 0.07 mm in HV ($P = 0.13$). The functional data were then preprocessed using different steps. We performed our analysis in the native space using the following steps. First, we performed a head-motion correction using rigid registration of functional brain volumes to the mean volumes of functional series. Second, we realigned the structural T1-weighted volume on the functional reference scan using Freesurfer (http://www.freesurfer.net/) and SPM (http://www.fil.ion.ucl.ac.uk/spm/) in the native functional space. Third, we reduced the physiological noise by applying the temporal CompCor method [Behzadi et al., 2007] with five principal components. The first step of CompCor is to determine noise regions of interest (ROIs; i.e., voxels with high temporal standard deviation). The first five principal components of the noise ROIs signal were selected. Then, we conducted global regression. The signal from the noise ROIs (white matter and cerebrospinal fluid) was used to model the physiological fluctuations in the gray matter. Fourth, we applied 5-mm spatial Gaussian smoothing in SPM.

Selection of ROI and Construction of Brain Functional Networks

According to an anatomical model [Alexander et al., 1986], we defined 182 ROIs to construct the associative, which includes the visual and auditory cortex, the limbic and the sensorimotor networks. The ROIs were selected from the parcellation obtained using Freesurfer software. Each network included the cortical areas and corresponding basal ganglia regions (caudate nucleus, putamen and globus pallidus), as well as the corresponding functional parts of the thalamus described by Worbe et al. [2012]. For each network, the anatomical labeling of the ROI is listed in the Supporting Information Table I. For each subject, we processed the anatomical T1-weighted images as follows. First, we obtained a cortical reconstruction using the spherical transformation provided by Freesurfer [Fischl et al., 1999, 2004]. The Freesurfer longitudinal registration process was used for the three sessions [Reuter et al., 2012] to take into account the longitudinal nature of study and to reduce the variability in morphology among the

sessions for the same subject. We created a template from these three sessions, which was the mean of the three T1 acquisitions. Since the parameters of all three acquisitions were the same for each subject, we applied linear registration using FLIRT in FSL software [Jenkinson and Smith, 2001; Jenkinson et al., 2002]. We defined ROIs corresponding to subcortical structures using the YeB atlas [Bardinet et al., 2009; Yelnik et al., 2007], a three-dimensional histological and deformable atlas of the basal ganglia. The YeB atlas was built from a single postmortem specimen that first was imaged with MRI and then processed for histology. A dedicated deformation strategy was set up and validated that allows the atlas to be accurately adapted to any brain through MR-based registration.

The functional network was built from this set of ROIs, which were represented as nodes interconnected by links. We calculated the mean time series across all voxels within each ROI in the individual space for each subject. We also computed individual correlation matrices between all pairs of ROIs within each functional circuit and subject. The edges represented the correlations between these time series.

We used the small-worldness coefficient to evaluate the small-world properties in the networks [Humphries and Gurney, 2008]. We calculated the small-world measures for each graph [Rubinov and Sporns, 2010]. These measures were designed for unweighted graphs and are highly dependent on graph cost, which corresponds to the graph's density (i.e., the proportion of actual connections regarding the total number of possible connections). To analyze the topological properties of brain functional networks, each correlation matrix was thresholded to create binary graphs. Many studies have presented methods for thresholding [e.g., De Vico Fallani et al., 2014], which remains a problematic step in small-world measures. To ensure that the topological measures were mathematically comparable across subjects, a common networks cost is necessary. Threshold functional connectivity matrices were thresholded successively over a range of network costs.

The topological results reported in this study are accordingly averages of the various metrics estimated for each individual network over the available cost range [Ginestet et al., 2011; Messé et al., 2013; Zalesky et al., 2012]. We then compared the average correlation maps among the HD, preHD and HV individuals. All of these analyses were performed on the whole network. However, since we defined three networks (i.e., sensorimotor, associative and limbic), where each one included the cortical areas and corresponding basal ganglia regions as well as corresponding functional parts of the thalamus, the graph theory metrics were averaged for each network.

Quantification of Functional Interactions

We quantified the large-scale functional connectivity organization of the three cortico-basal ganglia networks using graph theory metrics. *Graph theory* was applied to analyze

the fine-scale topological properties of each network. We calculated individual graph theory measures for each subject using the Brain Connectivity Toolbox (http://www.brain-connectivity-toolbox.net) [Rubinov and Sporns, 2010].

- L, the characteristic path length of the network, represents the average distance between node i and all other nodes:

$$L = \frac{1}{n} \sum_{i \in N} L_i = \frac{1}{n} \sum_{i \in N} \frac{\sum_{j \in N, \ j \neq i} d_{ij}}{n-1}$$

where N is the set of all nodes in the network and n is the number of nodes.
d_{ij} is the shortest path between i and j.

- k, the degree, represents the average connections of the node:

$$k_i = \sum_{j \in N} a_{ij}$$

- bc, the betweenness centrality, is the number of shortest paths between the nodes that pass through that a specific node i.

$$b_i = \frac{1}{(n-1)(n-2)} \sum_{h,i \in N} \frac{p_{hi}(i)}{P_{hi}}$$

- C, the clustering coefficient, represents the fraction of a node's neighbors that are also neighbors of one other.

$$C = \frac{1}{n} \sum_{i \in N} C_i = \frac{1}{n} \sum_{i \in N} \frac{2t_i}{k_i(k_i-1)}$$

The clustering coefficient and the local efficiency both represent the ability of a network to process specialized information within densely interconnected groups of nodes (functional segregation). The higher the clustering coefficient and local efficiency, the more segregated the network.

We first evaluated if the networks had small-world properties using the small-worldness coefficient (σ). A network was considered to have small-word properties if $\sigma > 1$ [Humphries and Gurney, 2008]:

$$\sigma = \frac{C/C_{\text{rand}}}{L/L_{\text{rand}}}$$

where C and C_{rand} are the clustering coefficients and L and L_{rand} are the characteristic path lengths of the tested network and random networks, respectively.

We also calculated the principal hubs, which are the nodes with a high number of connections (i.e., the highest degree k). The hubs facilitate integration between the parts of functional networks and ensure that the network is resilient against damage [Rubinov and Sporns, 2010]. We

identified the hubs using z-scores: A node was considered to be a hub if *hub index (Hi)*>1.

$$Hi = \frac{k - \bar{k}}{\delta(k)}$$

where k, the degree, represents the average connections of the node, $\bar{k}$ is the mean of k and $\delta(k)$ is the standard deviation of k.

Statistical Analysis

We conducted two-way, mixed ANOVA to determine the effect of Session (sessions 1–3) and Group (HV, preHD and HD) and the interaction Group × Session on graph theory measures first on the whole brain then on local circuits (associative, limbic and sensorimotor).

We assessed normality, homogeneity of variance and sphericity using Shapiro-Wilk, Levene's and Mauchly's tests, respectively.

Statistical significance of a simple two-way interaction and a simple main effect was accepted at a Bonferroni-adjusted alpha level of 0.025.

For each group (HD, preHD), each circuit (associative, limbic and sensorimotor) and each session (session 1–3), we computed the correlations between graph theory measures (k, bc, C) versus clinical scores (UHDRS), graph theory measures versus cognitive variables (SDMT and Stroop) and graph theory measures versus volumes of the subcortical regions of each circuit using Pearson's correlation coefficient. We adjusted the P-values for multiple comparisons using a permutations test [Nichols and Holmes, 2002].

RESULTS

We first compared the networks for global measures, and then we compared them for local measures in the associative, limbic and sensorimotor circuits.

Graph Theory Measures in the Whole Brain

No significant effect was found for the small-worldness coefficient (ó). There was a significant group effect for the average shortest path length (L, $P = 0.006$, Fig. 1, Table II). However, there were no session or interaction effects. L decreased in HD compared with the HV and with preHD individuals in sessions 1 and 2.

Graph Theory Measures in the Associative, Limbic and Sensorimotor Networks

Significant differences for local graph theory measures are presented in Figure 2 and Table II. The degree (k) differed among the groups in both the associative and limbic circuits. Post hoc comparisons revealed that k increased in HD patients in the associative network in session 1 compared with the HV and preHD individuals and in the limbic network compared with the HV and preHD
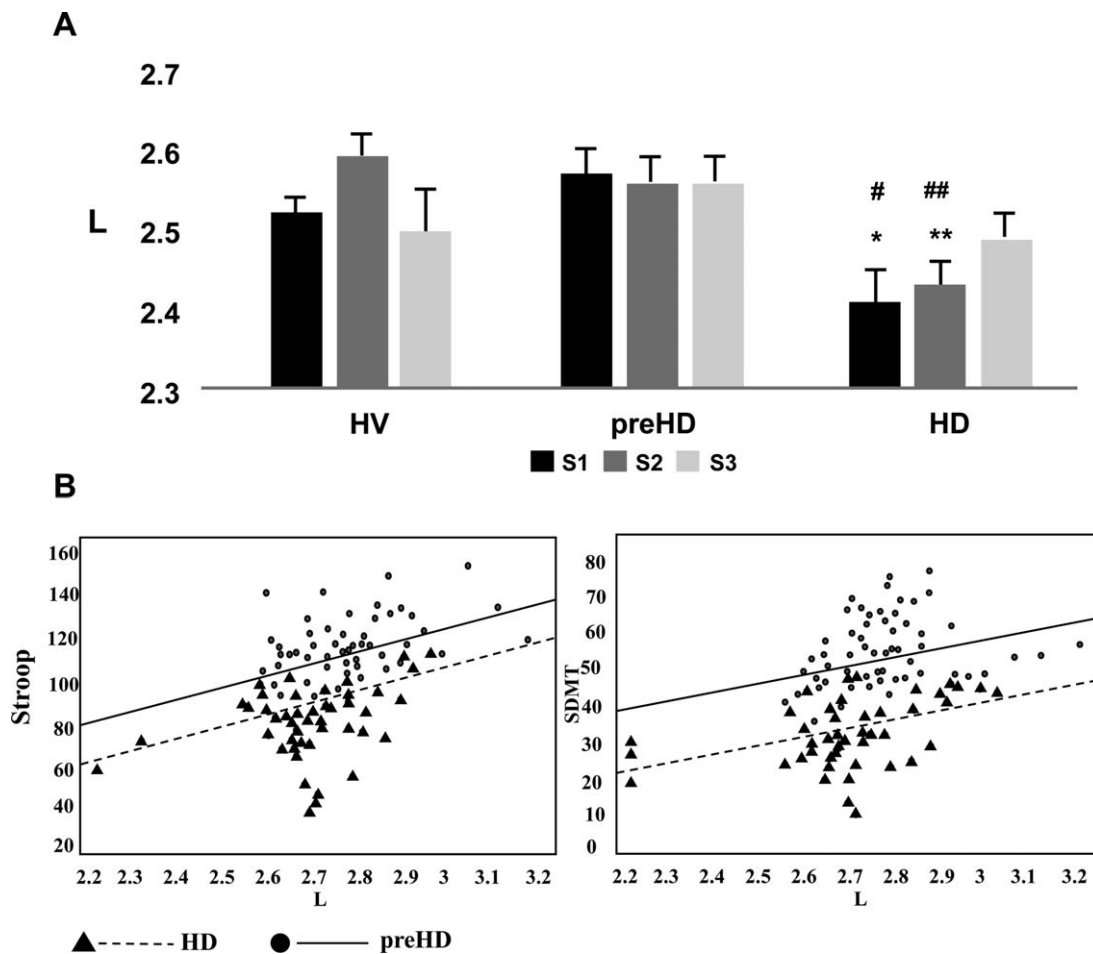
Figure 1.

Statistical analysis for graph theory measures in the whole brain. (**A**) Diagram showing changes in *L* in the three groups over the three sessions in the whole brain. There were significant between-group differences for the *L* metric (mixed-model ANOVA, $P = 0.006$) with a decrease in *L* in HD as compared with HV and preHD (post hoc *t*-test between HV and HD * $P < 0.05$, ** $P < 0.01$; post hoc *t*-test between HV and preHD # $P < 0.05$, ## $P < 0.01$ corrected for multiple comparisons). (**B**) Significant correlations between *L* and UHDRS in preHD (blue dots) and Stroop and SDMT in HD (red dots) and preHD.

individuals in all sessions. The betweenness centrality (*bc*) and the clustering coefficient (*C*) differed among groups in the sensorimotor network. Post hoc comparisons showed that *bc* decreased in HD patients compared with preHD patients in sessions 1 and 3 and that *C* decreased progressively from HV patients to HD patients with a decrease in HD patients compared with HV patients in all sessions and compared with the preHD individuals in session 2. No session or interaction effects were found for the graph theory measures in these three networks.

Graph Theory Measures in the Subcortical Regions

In the subcortical regions, *k* increased in the HD patients compared with the HV patients in the three circuits (Fig. 3

and Table II). In the associative circuit, there was a group effect with an increase in *k* in HD individuals compared with HV individuals in session 3 and with preHD patients in all sessions. There was also a session effect with an increase in *k* in HD patients from session 1 to session 3. In the limbic circuit, there was a group effect with an increase in *k* in HD patients compared with HV in sessions 1 and 3. In the sensorimotor circuit, there was a group effect as *k* increased in HD patients compared with HV and preHD individuals. Post hoc tests revealed that *k* increased in HD patients compared with HV and preHD individuals in sessions 1 and 3. *bc* decreased in the limbic and sensorimotor circuits in HD patients compared with preHD individuals. There was only a session effect in the basal ganglia (associative) for the degree measure *k* for HD patients. A session effect for *k* was found in the basal

TABLE II. Statistical analysis and graph theory measures in HV, preHD and HD for the whole brain and the three circuits (ANOVA mixed model)

Measure		HV	preHD	HD	ANOVA mixed model F value (P-value)	Post hoc t-test (P-value)	
Whole brain:							
L	S1	2.52 ± 0.02*	2.57 ± 0.03	2.41 ± 0.04	Group effect 5.47 (0.006)	*HV>HD in S1 ($P = 0.04$), S2 ($P = 0.002$)	
	S2	2.59 ± 0.03 *	2.56 ± 0.03#	2.43 ± 0.03*#	Session effect 0.58 (0.55)	#PreHD>HD in S1 ($P = 0.02$), S2 ($P = 0.009$)	
	S3	2.50 ± 0.05	2.56 ± 0.03#	2.49 ± 0.03#	Interaction 2.39 (0.05)		
C	S1	49.57 ± 0.58	50.59 ± 0.82	49.27 ± 0.83	Group effect 1.53 (0.22)		
$\times 10^2$	S2	50.73 ± 0.71	50.45 ± 0.71	48.88 ± 0.88	Session effect 1.29 (0.27)		
	S3	51.71 ± 0.83	50.27 ± 0.79	49.61 ± 0.72	Interaction 1.40 (0.23)		
	S1	3.944 ± 0.022	3.916 ± 0.030	4.138 ± 0.140	Group effect 1.29 (0.28)		
σ	S2	3.891 ± 0.024	3.902 ± 0.029	4.039 ± 0.120	Session effect 1.06 (0.34)		
	S3	4.216 ± 0.140	3.935 ± 0.034	3.975 ± 0.110	Interaction 2.22 (0.07)		
Cortex							
Associative network:							
k	S1	25.07 ± 0.33*	25.41 ± 0.33#	26.45 ± 0.28*#	Group effect 4.00 (0.02)	*HV<HD in S1 $P = 0.009$	
	S2	25.26 ± 0.29	25.26 ± 0.26	25.78 ± 0.24	Session effect 2.44 (0.09)	#PreHD<HD in S1 $P = 0.04$	
	S3	25.69 ± 0.40	25.72 ± 0.26	26.29 ± 0,30	Interaction 0.86 (0.48)		
Limbic network:							
k	S1	24.00 ± 0.39*	24.28 ± 0.30#	25.52 ± 0.33*#	Group effect 11.12 (0.00006)	*HV<HD in S1 ($P = 0.01$), S2 ($P = 0.03$), S3 ($P = 0.00003$)	
	S2	24.13 ± 0.47*	24.32 ± 0.51#	25.77 ± 0.43*#	Session effect 2.94 (0.05)	#PreHD<HD in S1 ($P = 0.01$), S2 ($P = 0.03$), S3 ($P = 0.003$)	
	S3	24.29 ± 0.36*	24.63 ± 0.57#	26.91 ± 0.38*#	Interaction 0.87 (0.47)		
Sensorimotor network:							
bc	S1	20.86 ± 0.41	21.35 ± 0.52 #	18.12 ± 1.1 #	Group effect 4.46 (0.01)	#PreHD>HD in S1 ($P = 0.04$), S3 ($P = 0.04$)	
$\times 10^4$	S2	21.32 ± 0.62	20.91 ± 0.61	19.23 ± 0.82	Session effect 0.95 (0.38)		
	S3	20.84 ± 0.11	22 ± 0.90 #	19.24 ± 0.91 #	Interaction 1.40 (0.23)		
C	S1	55.05 ± 0.92*	54.32 ± 1.35	52.21 ± 01.00*	Group effect 3.37 (0.03)	*HV>HD in S1 ($P = 0.01$), S2 ($P = 0.003$), S3 ($P = 0.004$)	
$\times 10^2$	S2	56.89 ± 1.15*	55.96 ± 1.25#	51.53 ± 1.07*#	Session effect 1.20 (0.30)	#PreHD>HD in S2 $P = 0.03$	
	S3	56.25 ± 1.03*	53.75 ± 1.28	52.82 ± 1.42*	Interaction 2.32 (0.05)		
Basal ganglia							
Associative network:							
k	S1	23.81 ± 0.82	23.12 ± 1.06#	26.03 ± 0.77#	Group effect 5.44 (0.006)	*HV<HD in S3 $P = 0.04$	
	S2	26.13 ± 1.12	23.47 ± 0.96#	27.48 ± 1.25#	Session effect 5.00 (0.007)	#PreHD<HD in S1 $P = 0.04$, S2 $P = 0.03$, S3 $P = 0.04$	
	S3	25.56 ± 1.03*	25.20 ± 1.18#	28.95 ± 1.18*#	Interaction 0.63 (0.63)	HD S1<S3 $P = 0.04$	
Limbic network:							
k	S1	20.26 ± 0.85*	20.85 ± 1.17	23.66 ± 0.83*	Group effect 3.54 (0.03)	HV<HD in S1 p=0.01 in S3 $P = 0.04$	
	S2	22.27 ± 0.9	21.03 ± 1.02	23.66 ± 128	Session effect 3.22 (0.04)		
	S3	23.12 ± 0.92	23.72 ± 1.21	25.32 ± 1.17	Interaction 1.03 (0.39)		
bc	S1	48.10 ± 0.21*	51.02 ± 0.21#	41.15 ± 0.22*#	Group effect 5.05 (0.008)	*HV>HD in S1 and S2 $P = 0.03$	

TABLE II. (continued).

Measure	HV	preHD	HD	ANOVA mixed model F value (P-value)	Post hoc t-test (P-value)	
$\times 10^3$	S2	$47.22 \pm 0.29^*$	$49.11 \pm 0.19\#$	$42.02 \pm 0.21^*\#$	Session effect 0.04 (0.95)	#PreHD>HD in S1 $P = 0.02$ in S2 $P = 0.03$ in S3 $P = 0.02$
	S3	49.02 ± 0.30	$49.09 \pm 0.28\#$	$42.06 \pm 0.29\#$	Interaction 0.13 (0.97)	
Sensorimotor network:						
k	S1	21.80 ± 0.91	$21.52 \pm 0.97\#$	$25.37 \pm 0.83\#$	Group effect 4.76 (0.01)	HV<HD in S1 $P = 0.01$ in S3 $P = 0.03$
	S2	24.27 ± 0.96	23.21 ± 1.06	25.56 ± 1.41	Session effect 3.35 (0.03)	#PreHD<HD in S1 =0.03 in S3 $P = 0.04$
	S3	23.56 ± 0.91	24.21 ± 1.16	27.12 ± 1.28	Interaction 0.52 (0.71)	
bc	S1	51.55 ± 2.49	$55.25 \pm 3.19\#$	$45.93 \pm 2.81\#$	Group effect 4.51 (0.01)	*HV>HD in S3 ($P = 0.04$)
$\times 10^3$	S2	52.60 ± 2.27	51.12 ± 2.77	51.57 ± 3.00	Session effect 0.33 (0.71)	# PreHD>HD in S1 and S3 ($P = 0.03$)
	S3	$53.61 \pm 4.58^*$	$61.82 \pm 4.78\#$	$44.37 \pm 2.13\#^*$	Interaction 0.88 (0.47)	

ganglia for the limbic and sensorimotor circuits, which was not found in the post hoc tests. No interaction effect was found for the graph theory measures in the subcortical regions.

Hubs in the Different Circuits

Using the Hi, we identified hubs in all of the groups (Fig. 4, Supporting Information Table II). Hi in the three circuits were 30.2, 30.4 and 31.7 in the associative circuit, 28.5, 28.4 and 29.0 in the limbic circuit, and 32.1, 33.1 and 32.6 in the sensorimotor circuit for S1, S2 and S3, respectively.

In the associative circuit, the hubs were located in the occipital cortex, left supramarginal gyrus (ROI 60, Brodmann area [BA] 18/19), left and right temporal planes of the superior temporal gyrus (ROI 70 and 144, respectively, BA 17), right lateral aspect of the superior temporal gyrus
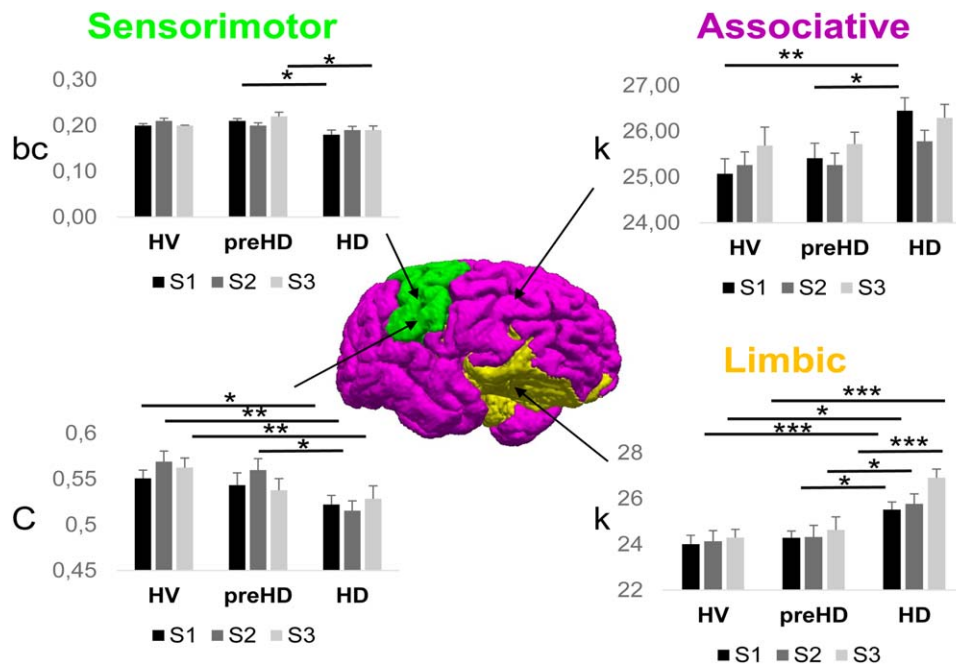

Figure 2.
Graph theory measures in the three circuits. Significant Group effects were observed for C ($P = 0.03$) and bc ($P = 0.01$) in the sensorimotor network, k in the associative ($P = 0.02$) and limbic network ($P = 0.00006$).
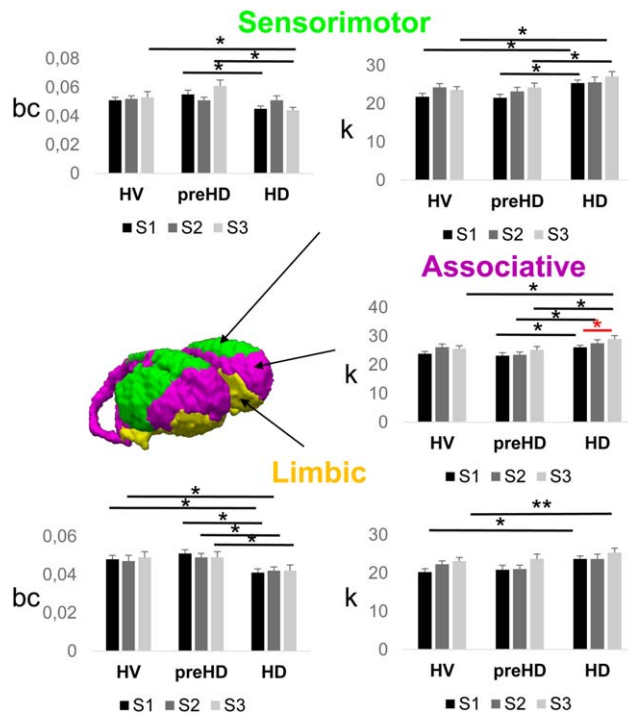
Figure 3.

Graph theory measures in the subcortical regions. Changes in (**A**) k in the sensorimotor network (group effect $P = 0.01$), and bc (group effect $P = 0.01$), (**B**) k in the associative subcortical regions (group effect $P = 0.0006$; session effect $P = 0.007$), (**C**) k in the limbic network (group effect $P = 0.03$) and the bc (group effect $P = 0.008$).

(ROI 142, BA 40/43), and right opercular part of the inferior gyrus (ROI 120, BA 40). In the limbic circuit, a hub was located in the right ventral putamen. In the sensorimotor circuit, hubs were located in the motor and premotor areas (BA 4/6), left subcentral gyrus and sulci (ROI 38), and left and right postcentral gyrus (ROI 62 and 137, respectively).

In the associative network, there was both a group and a session effect for Hi. The left supramarginal gyrus (ROI 60) and left and right temporal planes of the superior temporal gyrus (ROI 70 and 144) presented a session effect in HD patients, and ROI 70 presented a session effect in preHD patients. There was also a group effect indicating that the hubs were significantly reduced in preHD patients and no longer detectable in HD individuals (Supporting Information Table II).

In the limbic circuit, there was only a significant session effect in the right putamen in HD patients ($P = 0.04$), and post hoc t-tests revealed an increase in Hi in sessions 2 and 3 compared with session 1.

In the sensorimotor network, there was a group effect and no session effect. The hubs were significantly reduced in preHD individuals and no longer detectable in HD individuals (Supporting Information Table II). There was a

group effect for the following hubs: The left subcentral gyrus and sulci (ROI 38) and the left and right postcentral gyrus (ROI 62 and 137, respectively).

Clinical and Cognitive Variables

Significant differences for clinical and cognitive are presented in Table I. There was a session effect for UHDRS ($P = 0.0002$), and interaction session $\times$ group for SDMT ($P = 0.0007$) and a session ($P = 0.0005$) and an interaction session $\times$ group for the Stroop test ($P = 0.0006$). No significant post hoc t-tests were found only for the UHDRS in preHD individuals S1 < S3.

Correlation of Graph Theory Measures with Clinical and Cognitive Variables

L was correlated with CAG repeat size in preHD individuals and with the SDMT and the Stroop test in preHD and HD patients (Fig. 1, Table III).

Correlations between clinical scores versus graph theory measures and cognitive scores versus graph theory measures in cortical regions for each network are presented in Figure 5 and Table III. In HD patients, we found that UHDRS scores were positively correlated with k in the associative and limbic circuits; the Stroop and SDMT tests were negatively correlated with k in the associative and
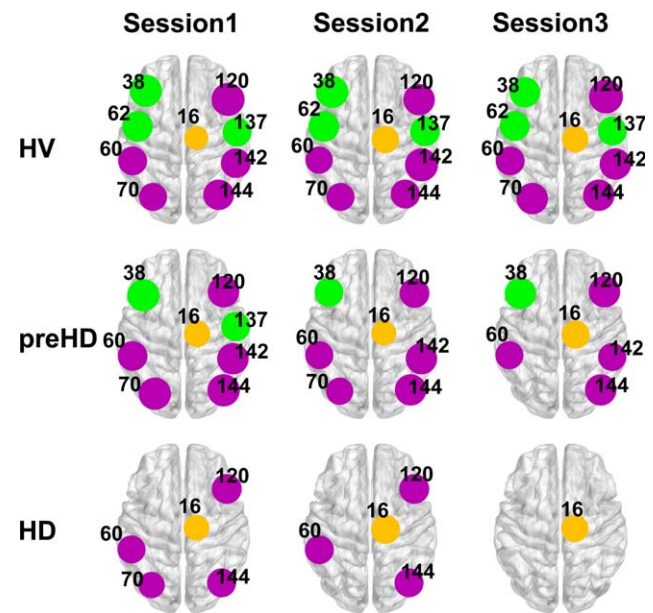

Figure 4.

Changes in hub organization in the three circuits. In the sensorimotor network (green dots), there were a significant group effect, hubs were reduced in preHD and no longer detectable in HD. In the associative network (pink dots), there was both a group and a session effect. In the limbic network (yellow dots), there was a significant session effect in the right putamen in HD patients ($P = 0.04$).

limbic circuits. No other correlations were found. In preHD individuals, UHDRS scores were negatively correlated with L and C in the sensorimotor circuit and positively correlated with k in the associative circuit. The SDMT and Stroop test scores were positively correlated with L and C in the sensorimotor circuit.

Correlations between the clinical and cognitive variables and the graph theory measures in the subcortical regions for each network are presented in Figure 6 and Table III. We only found correlations for C in preHD individuals. In the associative and sensorimotor circuits, C was negatively correlated with UHDRS score. In the limbic circuit, C was positively correlated with Stroop test score.

Correlations between the burden score and graph theory measures in preHD patients were observed in the sensorimotor circuit only (Fig. 6, Table III). The burden score was negatively correlated with bc and k in both the cortical and subcortical regions.

Correlation of Graph Theory Measures with Basal Ganglia Volume

Correlations among basal ganglia volume and graph theory measures are presented in Supporting Information Table III.

The total volume of the limbic subdivision of the basal ganglia (including the limbic putamen, caudate and globus pallidus, as defined by the YeB atlas) was negatively correlated with the measure k for the limbic basal ganglia in HD patients. The total volume of the sensorimotor subdivision of the basal ganglia (including the sensorimotor putamen, caudate and globus pallidus of the basal ganglia) was positively correlated with C for the sensorimotor basal ganglia in HD individuals.

The volumes of the left external globus pallidus (associative), right putamen (limbic) and left putamen (sensorimotor) were positively correlated with k in HD individuals. The volume of the left caudate (associative) was negatively correlated with k in HD patients. The volumes of the left and right external globus pallidus (sensorimotor) and the volumes of the left and right putamen (associative) were positively correlated with C in HD individuals.

The volume of the right external globus pallidus (sensorimotor) was negatively correlated with bc in HD patients and positively correlated with bc in preHD individuals. The volume of the left external globus pallidus (sensorimotor) was negatively correlated with bc in preHD patients.

DISCUSSION

The aim of our study was to investigate longitudinally the functional alterations in brain connectivity in HD and preHD individuals. The main results can be summarized as follows: HD patients exhibited a reduced average shortest path length (L), which indicated a reduction in the small-world network organization of the brain, whose

TABLE III. Correlation between UHDRS, SDMT, Stroop and graph theory measures

Measure	Variable	preHD r	preHD P-value	HD r	HD P-value
Whole brain					
L	SDMT	0.27	0.02	0.36	0.007
	Stroop	0.38	0.0009	0.38	0.004
Cortex					
Associative network					
k	UHDRS	0.30	0.002	0.28	0.03
	SDMT			−0.36	0.007
	Stroop			−0.39	0.003
Limbic network					
k	UHDRS			0.38	0.004
	SDMT			−0.22	0.04
	Stroop			−0.31	0.02
Sensorimotor network					
C	UHDRS	−0.36	0.001		
	SDMT	0.22	0.03		
	Stroop	0.27	0.01		
bc	Burden	−0.35	0.001		
k	Burden	−0.36	0.00		
Basal ganglia					
Associative network					
C	UHDRS	−0.35	0.002		
Limbic network					
C	Stroop	0.27	0.02		
Sensorimotor network					
C	UHDRS	−0.32	0.005		
k	Stroop	0.25	0.03		
	Burden	−0.32	0.002		
bc	Stroop	−0.21	0.03		
	Burden	−0.27	0.01		

topology tended to approximate that of a random network. The nodes in HD patients were also more connected (increased in k), had fewer short paths between them (reduced bc) and their neighbors were less frequently neighbors of one other (reduced C). Changes predominated in the sensorimotor network for bc and C and were observed in all circuits for k. Conversely, preHD subjects showed no changes in graph theory measures with the exception of the hubs. Overall, the hubs were reduced in preHD individuals and no longer detectable in HD patients in the sensorimotor and associative networks. Changes in graph theory measures correlated variably with clinical and cognitive measures. Lastly, there were no changes in graph theory measures across sessions, which suggests that these measures are not reliable biomarkers of longitudinal changes in HD.

Graph Theory Measures in HD Patients

This investigation represents the first longitudinal study evaluating functional connectivity in HD over two years of
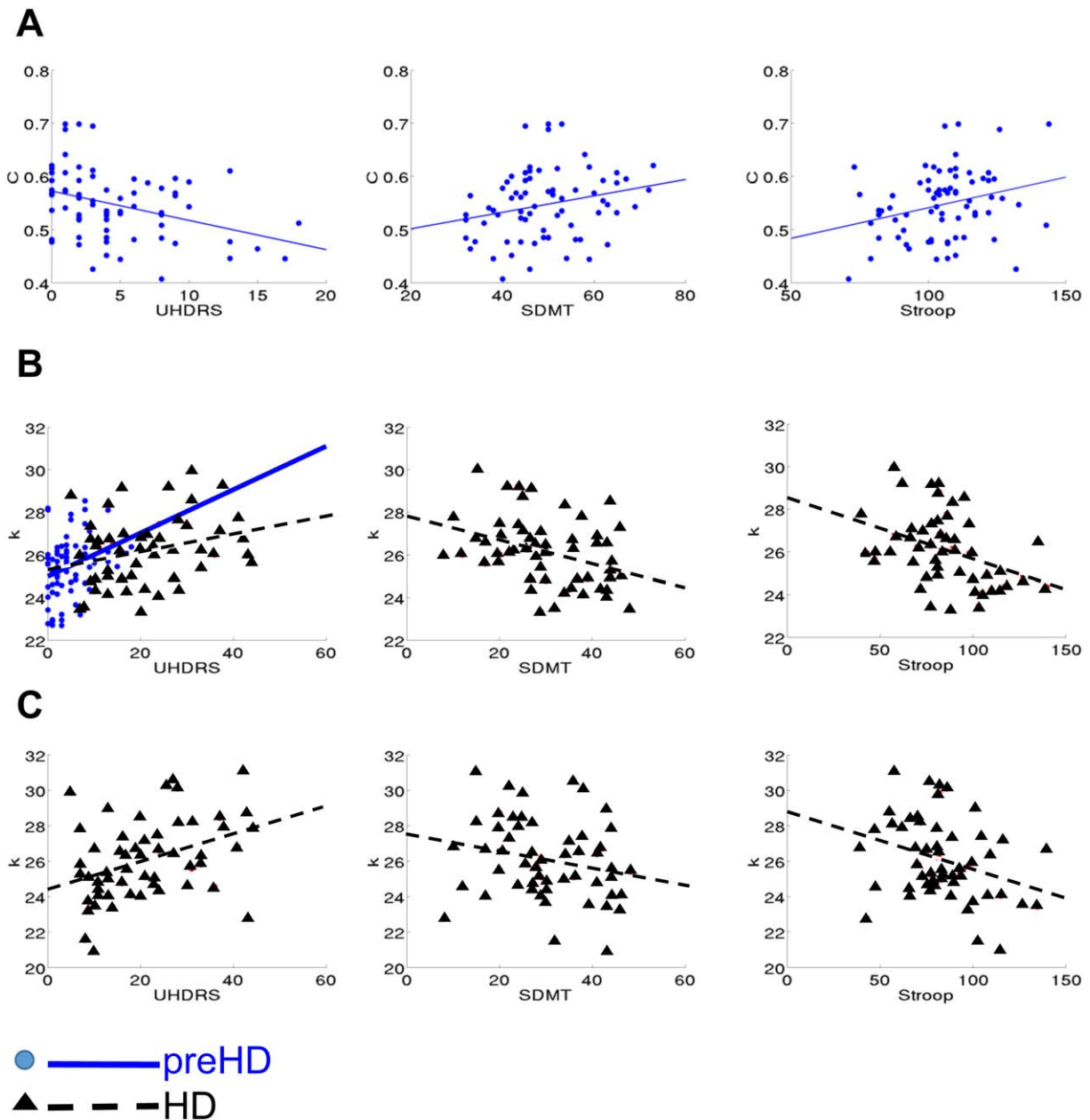
Figure 5.

Correlations between graph theory measures and clinical, cognitive variables for each circuit. (**A**) Sensorimotor circuit: correlation between C and scores at the UHDRS, SDMT and Stroop in preHD. (**B**) Associative circuit: correlation between k and scores at the UHDRS, SDMT and Stroop in HD, and UHDRS in follow-up. The average shortest path length (*L*) decreased in patients (significant group effect), which indicated that the topology of the pathological network was similar to that of a random network topology. For local measures, nodes in HD individuals exhibited increases in *k*, which preHD. (**C**) Limbic circuit: correlation between k and scores at the UHDRS, SDMT and Stroop in HD patients. PreHD subjects are represented by blue dots and HD patients by red dots. Values are presented in Table III. [Color figure can be viewed at wileyonlinelibrary.com]

attests to the sparsity of the network, reduced *bc* (i.e., fewer short paths) and reduced *C*. These data, which relate to the neighborhood density of a node, quantify the local connectivity. An increase in *k* may indicate that more regions were operating at the same time in HD patients. Individuals
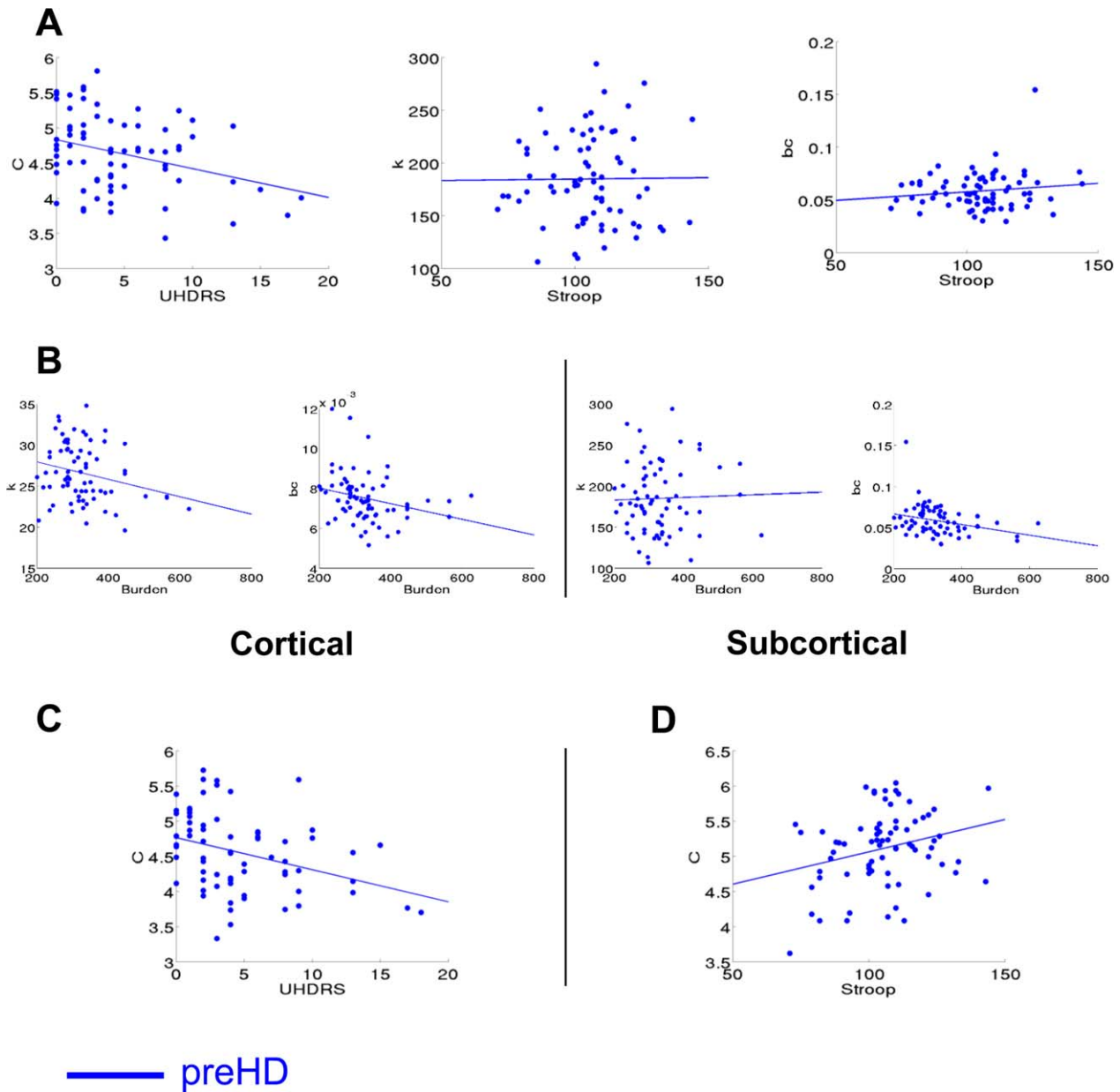
Figure 6.

Correlations between graph theory measures clinical and cognitive variables of basal ganglia. (**A**) Sensorimotor circuit: correlations between C and scores at the UHDRS, k, bc and Stroop in preHD. (**B**) Sensorimotor circuit: correlations between bc, k and burden for cortical regions and subcortical regions in preHD. (**C**) Associative circuit: correlation between C and scores at the UHDRS in preHD. (**D**) Limbic circuit: correlation between C and scores at the Stroop in preHD. PreHD subjects are represented by blue dots and HD patients by red dots. [Color figure can be viewed at wileyonlinelibrary.com]

suffering from HD also demonstrated a disappearance of hubs in their associative and sensorimotor circuits. Overall, the functional connectivity for HD patients was characterized by a reduced performance compared with that of HV.

Comparing our results with those reported in previous studies is difficult because the definition of functional connectivity depends on the method used. The majority of previous studies used seed-based approaches and independent component analysis to measure functional connectivity. These methods only provide information about the strength of the functional synchronization between distant regions. Reduced functional connectivity has been

reported by numerous studies in multiple brain networks in HD individuals. This reduction in connectivity was extensive and affected multiple networks. A reduction between frontal regions and the medial visual network has been reported [Dumas et al., 2013] in the default mode network [Dumas et al., 2013; Quarantelli et al., 2013], the executive control network [Dumas et al., 2013], the dorsal attentional network [Poudel et al., 2014], in parietal regions [Werner et al., 2014], and between the posterior putamen, the superior parietal and the frontal executive network [Poudel et al., 2014]. Our study, which confirms that changes are widespread involving the sensorimotor, associative and limbic networks, complements these findings by demonstrating that changes predominated in the sensorimotor network (for bc and C). In contrast, only a few studies have reported increased connectivity in the left fronto-parietal network [Poudel et al., 2014; Werner et al., 2014], the thalamus, striatum and default mode network [Werner et al., 2014]. The reason for this discrepancy is not known and has been interpreted as indicating the reduced ability of intranetwork differentiation [Werner et al., 2014].

Graph Theory Measures in preHD Subjects

In contrast with HD patients, local graph theory metrics (k, C, bc) were largely maintained in preHD subjects. This finding is consistent with the results of a previous study [Harrington et al., 2015]. PreHD subjects only exhibited a reduction in the number of hubs in the three circuits. Using independent component analysis or seed-based approaches, previous studies found variable changes in functional connectivity in preHD subjects. Reductions have been reported between the premotor cortex and caudate nucleus [Koenig et al., 2014], the visual network and frontal areas [Dumas et al., 2013; Unschuld et al., 2012], the default mode network [Unschuld et al., 2012] and the dorsal attentional network [Poudel et al., 2014].

Only one study used graph theory to compare functional connectivity in preHD patients classified into low, medium and high subgroups depending on burden score [Harrington et al., 2015]. These authors used graph theory measures similar to ours: The global efficiency, which corresponds to the average inverse shortest path length (L), the clustering coefficient and the density [Latora and Marchiori, 2001; Rubinov and Sporns, 2010]. Consistent with a previous study [Harrington et al., 2015], we did not find significant changes in density (data not shown). This study reported an increase in global efficiency (equivalent to a decrease in L) in medium and advanced preHD subjects (high burden score). This finding is consistent with our results in HD subjects. In contrast, we failed to detect changes in L in preHD individuals. This negative finding may be explained by the fact that we included fewer preHD subjects with younger ages corresponding to the low and medium groups of Harrington et al. [2015]. In our study, hubs were reduced in preHD individuals in the

associative and sensorimotor circuits, which is consistent with the decrease in the rich club organization in the medium and high preHD groups reported previously [Harrington et al., 2015]. The rich club metric is similar to the brain hubs in our study [van den Heuvel and Sporns, 2011]. Together, these results suggest that preHD is characterized by progressive changes in global network interconnectivity, whose network topology becomes more random, and decreased hub organization as a diagnosis of HD approaches. These changes worsen in HD patients; changes in local metrics are observed later in HD patients.

Graph Theory Measures in Associative, Limbic and Sensorimotor Networks (Cortical and Subcortical)

In HD, reduction in hubs was observed in the sensorimotor network in all sessions, but the associative hubs were maintained during the first and second sessions. In HD, most functional imaging studies have reported reduced functional connectivity at rest within motor areas as well as associative areas of the frontal and parietal lobes [Dumas et al., 2013; Poudel et al., 2014] and the default mode network [Dumas et al., 2013]. We complement these results by showing that changes predominated in the sensorimotor network, as suggested by changes in bc and C. However, we note that changes in k were observed in all of the circuits.

Longitudinal Changes in Graph Theory Measures

Overall, there were little or no changes in the graph theory metrics across sessions in either the preHD or the HD objects. This finding is consistent with previous studies of preHD subjects that failed to demonstrate changes in functional connectivity using independent component analysis [Odish et al., 2015] or seed-based analysis in the isthmus of the cingulate region and the putamen [Seibert et al., 2012]. These two longitudinal studies investigated preHD patients and assessed the potential utility of rs-fMRI as a biomarker of disease progression. The authors did not find significant changes in connectivity after one year [Seibert et al., 2012] or three years of follow-up [Odish et al., 2015]. Taken together, these results suggest that functional connectivity measures using rs-fMRI may not provide good markers of disease progression. This results may be due to the wide range of possible strategies for data analysis that can influence the results of graph theory calculation, including the choice of graph thresholding, the number of cortical and subcortical regions and the size of the sample, as shown previously [Vives-Gilabert et al., 2013]. In addition, the results of graph theory metrics based on task fMRI have demonstrated significant between-subject variability [Vives-Gilabert et al., 2013].

In contrast to global or local connectivity measures (C, bc), there was a significant increase in k (indicating increased node connections) in subcortical regions for the

three circuits in HD individuals compared with the controls. In some cases, this finding was correlated with their reduction in volume. In HD patients, the increase in k was more pronounced in the associative circuit than in other circuits, as shown by the presence of a session effect.

Lastly, there were significant changes in hub organization over time. We noted a reduction in hubs in the associative circuits in HD individuals (session effect in BA 18/19 and 17) and in preHD subjects (BA 17).

The lack of longitudinal changes in imaging data was not related to the absence of clinical decline. We can conclude that three years may not be sufficient for a longitudinal study related to HD.

Correlation of Graph Theory Measures with Clinical and Cognitive Variables

We found that the graph theory measures correlated to differing degrees with the clinical measurements. Diminished performances on clinical tests were associated with a decreased path length L, an increased degree k and a reduced clustering C. In HD, there was some degree of circuit specificity between graph theory and clinical measures. Correlations with apathy scores were observed in the limbic network, and correlations with cognitive tests (SDMT and Stroop) were observed in the associative network. In contrast, UHDRS scores were correlated with k in the associative and limbic network but not in the sensorimotor network, as expected. In addition, a decrease in L was also correlated with reduced performance on the SDMT and Stroop tests. This circuit specificity was not obvious in preHD individuals; C in the sensorimotor and limbic networks was correlated with all tests. We found that the UHDRS scores were correlated with graph theory measures in all of the networks. The correlations furthermore did not appear consistent across the studies, and no correlation was found between scores on the Stroop test and the tail making test in preHD individuals, unlike the results of a previous study [Harrington et al., 2015]. Lastly, the burden score was correlated with graph theory measures in the cortical and subcortical regions, which is consistent with the results of Harrington et al. [2015], but in the sensorimotor network only. Together with the predominance of changes in graph theory metrics in the sensorimotor network, this findings suggests that the disease process has a larger impact on the sensorimotor network connectivity.

LIMITATIONS

The study included only a moderate number of subjects. More changes may have been detected in preHD individuals had we used a larger number of subjects. The head motion of the patients might also have affected the rs-fMRI measures [Van Dijk et al., 2012] despite the motion-correction procedures applied to the data [Power et al.,

2014]. Head movements are particularly expected in HD subjects. To regress out movement-induced variance, we included motion-realignment parameters in our analysis. The variance of the realignment parameters of patients did not significantly differ from that of the controls. We also excluded TRACK-HD subjects with excessive movement.

CONCLUSION

In this study, we demonstrated global and fine-scale functional disorganization of cortico-basal ganglia networks in HD. This functional disorganization may reflect the disorganization of cortico-basal ganglia networks, with progressive loss of some small-world properties and loss of hubs predominating in the sensorimotor and associative networks. Moreover, our data also partly support the hypothesis that the dysfunction of different networks might contribute to the clinical heterogeneity of HD. In conclusion, preHD is characterized by progressive decreasing hub organization, and these changes worsen in HD patients with changes in local metrics. HD is characterized by progressive changes in global network interconnectivity that render the network topology more random over time.

We observed correlations between the burden score and graph theory measures for preHD in the sensorimotor circuit only. The burden score was negatively correlated with bc and k in both the cortical and subcortical regions.

ACKNOWLEDGMENT

REFERENCES

Alexander GE, DeLong MR, Strick PL (1986): Parallel organization of functionally segregated circuits linking basal ganglia and cortex. Annu Rev Neurosci 9:357–381. doi:10.1146/annurev.ne.09.030186.002041

Bardinet E, Bhattacharjee M, Dormont D, Pidoux B, Malandain G, Schüpbach M, Ayache N, Cornu P, Agid Y, Yelnik J (2009): A three-dimensional histological atlas of the human basal ganglia. II. Atlas deformation strategy and evaluation in deep brain stimulation for Parkinson disease. J Neurosurg 110:208–219. doi:10.3171/2008.3.17469

Behzadi Y, Restom K, Liau J, Liu TT (2007): A component based noise correction method (CompCor) for BOLD and perfusion based fMRI. NeuroImage 37:90–101. doi:10.1016/j.neuroimage.2007.04.042

Bullmore E, Sporns O (2009): Complex brain networks: Graph theoretical analysis of structural and functional systems. Nat Rev Neurosci 10:186–198. doi:10.1038/nrn2575

Bullmore E, Sporns O (2012): The economy of brain network organization. Nat Rev Neurosci 13:336–349. doi:10.1038/nrn3214

Damoiseaux JS, Greicius MD (2009): Greater than the sum of its parts: A review of studies combining structural connectivity and resting-state functional connectivity. Brain Struct Funct 213:525–533. doi:10.1007/s00429-009-0208-6

De Vico Fallani F, Richiardi J, Chavez M, Achard S (2014): Graph analysis of functional brain networks: Practical issues in translational neuroscience. Philos Trans B Biol Sci 369:20130521. doi:10.1098/rstb.2013.0521

Delmaire C, Dumas EM, Sharman MA, van den Bogaard SJA, Valabregue R, Jauffret C, Justo D, Reilmann R, Stout JC, Craufurd D, Tabrizi SJ, Roos RAC, Durr A, Lehéricy S (2013): The structural correlates of functional deficits in early huntington's disease. Hum Brain Mapp 34:2141–2153.

Dumas EM, van den Bogaard SJA, Hart EP, Soeter RP, van Buchem MA, van der Grond J, Rombouts SARB, Roos RAC (2013): Reduced functional brain connectivity prior to and after disease onset in Huntington's disease. NeuroImage Clin 2: 377–384. doi:10.1016/j.nicl.2013.03.001

Dumas LJ, O'Bleness MS, Davis JM, Dickens CM, Anderson N, Keeney JG, Jackson J, Sikela M, Raznahan A, Giedd J, Rapoport J, Nagamani SSC, Erez A, Brunetti-Pierri N, Sugalski R, Lupski JR, Fingerlin T, Cheung SW, Sikela JM (2012): DUF1220-Domain Copy Number Implicated in Human Brain-Size Pathology and Evolution. Am J Hum Genet 91:444–454. doi:10.1016/j.ajhg.2012.07.016

Fischl B, Sereno MI, Dale AM (1999): Cortical surface-based analysis. II: Inflation, flattening, and a surface-based coordinate system. NeuroImage 9:195–207. doi:10.1006/nimg.1998.0396

Fischl B, van der Kouwe A, Destrieux C, Halgren E, Ségonne F, Salat DH, Busa E, Seidman LJ, Goldstein J, Kennedy D, Caviness V, Makris N, Rosen B, Dale AM (2004): Automatically parcellating the human cerebral cortex. Cereb Cortex 1991 14:11–22.

Fornito A, Zalesky A, Breakspear M (2015): The connectomics of brain disorders. Nat Rev Neurosci 16:159–172. doi:10.1038/nrn3901

Ginestet CE, Nichols TE, Bullmore ET, Simmons A (2011): Brain network analysis: Separating cost from topology using cost-integration. PLoS One 6.doi:10.1371/journal.pone.0021570

Greicius MD, Supekar K, Menon V, Dougherty RF (2009): Resting-state functional connectivity reflects structural connectivity in the default mode network. Cereb Cortex 19:72–78. doi:10.1093/cercor/bhn059

Harrington DL, Rubinov M, Durgerian S, Mourany L, Reece C, Koenig K, Bullmore E, Long JD, Paulsen JS, Rao SM, PREDICT-HD Investigators of the Huntington Study Group (2015): Network topology and functional connectivity disturbances precede the onset of Huntington's disease. Brain J Neurol 138: 2332–2346., doi:10.1093/brain/awv145

Humphries MD, Gurney K (2008): Network "small-world-ness": A quantitative method for determining canonical network equivalence. PLoS One 3:e0002051. doi:10.1371/journal.pone.0002051

Jenkinson M, Smith S (2001): A global optimisation method for robust affine registration of brain images. Med Image Anal 5: 143–156.

Jenkinson M, Bannister P, Brady M, Smith S (2002): Improved optimization for the robust and accurate linear registration and motion correction of brain images. NeuroImage 17:825–841.

Kaiser M, Hilgetag CC (2006): Nonoptimal component placement, but short processing paths, due to long-distance projections in neural systems. PLoS Comput Biol 2:e95. doi:10.1371/journal.pcbi.0020095

Koenig KA, Lowe MJ, Harrington DL, Lin J, Durgerian S, Mourany L, Paulsen JS, Rao SM (2014): Functional connectivity of primary motor cortex is dependent on genetic burden in prodromal Huntington disease. Brain Connect 4:535–546. doi:10.1089/brain.2014.0271

Latora V, Marchiori M (2001): Efficient behavior of small-world networks. Phys Rev Lett 87:198701. doi:10.1103/PhysRevLett.87.198701

Majid DSA, Aron AR, Thompson W, Sheldon S, Hamza S, Stoffers D, Holland D, Goldstein J, Corey-Bloom J, Dale AM (2011): Basal ganglia atrophy in prodromal Huntington's disease is detectable over one year using automated segmentation. Mov Disord 26:2544–2551. doi:10.1002/mds.23912

Messé A, Caplain S, Pélégrini-Issac M, Blancho S, Lévy R, Aghakhani N, Montreuil M, Benali H, Lehéricy S (2013): Specific and evolving resting-state network alterations in post-concussion syndrome following mild traumatic brain injury. PLoS One 8:e65470. doi:10.1371/journal.pone.0065470

Nichols TE, Holmes AP (2002): Nonparametric permutation tests for functional neuroimaging: A primer with examples. Hum Brain Mapp 15:1–25.

Odish OFF, van den Berg-Huysmans AA, van den Bogaard SJA, Dumas EM, Hart EP, Rombouts SARB, van der Grond J, Roos RAC, on behalf of the TRACK-HD Investigator Group (2015): Longitudinal resting state fMRI analysis in healthy controls and pre-manifest Huntington's disease gene carriers: A three-year follow-up study. Hum Brain Mapp 36:110–119.

Penney JB, Vonsattel JP, Macdonald ME, Gusella JF, Myers RH (1997): CAG repeat number governs the development rate of pathology in Huntington's disease. Ann Neurol 41:689–692. doi:10.1002/ana.410410521

Poudel GR, Egan GF, Churchyard A, Chua P, Stout JC, Georgiou-Karistianis N (2014): Abnormal synchrony of resting state networks in premanifest and symptomatic Huntington disease: The IMAGE-HD study. J Psychiatry Neurosci 39:87–96. doi:10.1503/jpn.120226

Power JD, Mitra A, Laumann TO, Snyder AZ, Schlaggar BL, Petersen SE (2014): Methods to detect, characterize, and remove motion artifact in resting state fMRI. NeuroImage 84: 320–341. doi:10.1016/j.neuroimage.2013.08.048

Quarantelli M, Salvatore E, Giorgio SMDA, Filla A, Cervo A, Russo CV, Cocozza S, Massarelli M, Brunetti A, De Michele G (2013): Default-mode network changes in Huntington's disease: An integrated MRI study of functional connectivity and morphometry. PLoS One 8:e72159. doi:10.1371/journal.pone.0072159

Reuter M, Schmansky NJ, Rosas HD, Fischl B (2012): Within-subject template estimation for unbiased longitudinal image analysis. NeuroImage 61:1402–1418. doi:10.1016/j.neuroimage.2012.02.084

Rosas HD, Hevelone ND, Zaleta AK, Greve DN, Salat DH, Fischl B (2005): Regional cortical thinning in preclinical Huntington disease and its relationship to cognition. Neurology 65: 745–747. doi:10.1212/01.wnl.0000174432.87383.87

Ross CA, Tabrizi SJ (2011): Huntington's disease: From molecular pathogenesis to clinical treatment. Lancet Neurol 10:83–98. doi:10.1016/S1474-4422(10)70245-3

Rubinov M, Sporns O (2010): Complex network measures of brain connectivity: Uses and interpretations. NeuroImage 52: 1059–1069. doi:10.1016/j.neuroimage.2009.10.003

Seibert TM, Majid DSA, Aron AR, Corey-Bloom J, Brewer JB (2012): Stability of resting fMRI interregional correlations analyzed in subject-native space: A one-year longitudinal study in healthy adults and premanifest Huntington's disease. Neuroimage 59:2452–2463. doi:10.1016/j.neuroimage.2011.08.105

Smith A (1982): Symbol Digit Modalities Test (SDMT) Manual (Revised) Western Psychological Services. Los Angeles.

Stroop JR (1935): Studies of interference in serial verbal reactions. J Exp Psychol 18:643–662.

Tabrizi SJ, Langbehn DR, Leavitt BR, Roos RA, Durr A, Craufurd D, Kennard C, Hicks SL, Fox NC, Scahill RI, Borowsky B, Tobin AJ, Rosas HD, Johnson H, Reilmann R, Landwehrmeyer B, Stout JC, TRACK-HD Investigators (2009): Biological and clinical manifestations of Huntington's disease in the longitudinal TRACK-HD study: Cross-sectional analysis of baseline data. Lancet Neurol 8:791–801. doi:10.1016/S1474-4422(09)70170-X

Teichmann M, Dupoux E, Kouider S, Brugières P, Boissé MF, Baudic S, Cesaro P, Peschanski M, Bachoud-Lévi AC (2005): The role of the striatum in rule application: The model of Huntington's disease at early stage. Brain 128:1155–1167. doi:10.1093/brain/awh472

Unified Huntington's Disease Rating Scale: Reliability and Consistency. Huntington Study Group (1996): Mov Disord 11: 136–142. doi:10.1002/mds.870110204

Unschuld PG, Joel SE, Liu X, Shanahan M, Margolis RL, Biglan KM, Bassett SS, Schretlen DJ, Redgrave GW, van Zijl PCM, Pekar JJ, Ross CA (2012): Impaired cortico-striatal functional connectivity in prodromal Huntington's Disease. Neurosci Lett 514:204–209. doi:10.1016/j.neulet.2012.02.095

van den Heuvel MP, Sporns O (2011): Rich-club organization of the human connectome. J Neurosci 31:15775–15786. doi: 10.1523/JNEUROSCI.3539-11.2011

Van Dijk KRA, Sabuncu MR, Buckner RL (2012): The influence of head motion on intrinsic functional connectivity MRI. NeuroImage 59:431–438. doi:10.1016/j.neuroimage.2011.07.044

Vives-Gilabert Y, Abdulkadir A, Kaller CP, Mader W, Wolf RC, Schelter B, Klöppel S (2013): Detection of preclinical neural dysfunction from functional connectivity graphs derived from task fMRI. An example from degeneration. Psychiatry Res 214: 322–330. doi:10.1016/j.pscychresns.2013.09.009

Vonsattel JPG (2008): Huntington disease models and human neuropathology: Similarities and differences. Acta Neuropathol 115:55–69. doi:10.1007/s00401-007-0306-6

Werner CJ, Dogan I, Saß C, Mirzazade S, Schiefer J, Shah NJ, Schulz JB, Reetz K (2014): Altered resting-state connectivity in Huntington's disease. Hum Brain Mapp 35:2582–2593.

Worbe Y, Malherbe C, Hartmann A, Pélégrini-Issac M, Messé A, Vidailhet M, Lehéricy S, Benali H (2012): Functional immaturity of cortico-basal ganglia networks in Gilles de la Tourette syndrome. Brain J Neurol 135:1937–1946. doi:10.1093/brain/aws056

Yelnik J, Bardinet E, Dormont D, Malandain G, Ourselin S, Tandé D, Karachi C, Ayache N, Cornu P, Agid Y (2007): A three-dimensional, histological and deformable atlas of the human basal ganglia. I. Atlas construction based on immunohistochemical and MRI data. NeuroImage 34:618–638. doi:10.1016/j.neuroimage.2006.09.026

Zalesky A, Cocchi L, Fornito A, Murray MM, Bullmore E (2012): Connectivity differences in brain networks. NeuroImage 60: 1055–1062. doi:10.1016/j.neuroimage.2012.01.068